

Numerical Investigation of Jet and Vortex Actuator (JaVA) for Active Flow Control

Sertac Cadirci¹ and Hasan Gunes²
Istanbul Technical University, Istanbul, Turkey, 34437

Ulrich Rist³
Universität Stuttgart, Stuttgart, Baden-Württemberg, D-70550, Germany

An oscillatory, zero-net-mass flux Jet and Vortex Actuator (JaVA) was modelled as part of a flat plate and simulated in a boundary layer flow. JaVA is an active flow control device that can be used for flow separation control and thus can delay boundary layer transition. It has been already shown experimentally that JaVA induced flow types in still water include angled and vertical jets, wall jets and vortex flows and that they highly depend on governing parameters such as the frequency and amplitude of the actuator and the mean position of the actuator plate. In this study, a commercial unsteady, incompressible Navier-Stokes solver (Fluent) has been used to study the flow fields generated by JaVA in a water channel. The detailed quantitative information about the performance of JaVA on a flat plate boundary layer is obtained numerically. The results are validated by visualization experiments with the similar CFD set up. The numerical results show vortex like structures emerging from actuator's wide gap with a size that matches the experimentally observed vortex. It has been found that the emerging vortices move along the flat plate surface usually merging with each other downstream of the boundary layer. In addition to governing JaVA parameters in still water (the jet Reynolds number, the scaled amplitude, the mean position of the actuator), the characteristics of boundary layer flow are important for the JaVA performance in channel flow. These include the magnitude of the free stream velocity and the boundary layer profile (e.g. laminar or turbulent). In this study, we consider an approximation to the Blasius profile (a 4th-order polynomial profile). To account the free stream velocity, a new dimensionless parameter (r) is introduced which is the ratio of average jet velocity " $V_j = 2abf / w_w$ " to free stream velocity " U_∞ " ($r = V_j / U_\infty$). Our numerical results clearly show that JaVA, when mounted in a flat plate laminar boundary layer, affects boundary layer profile considerably. That is, JaVA induced boundary layer profiles are clearly more resistant to the flow separation. The effects of JaVA with different operation regimes on the various boundary layer flow characteristics such as the displacement thickness, the momentum thickness, the energy thickness and the friction coefficient are reported. This computational study can be utilized to steer the governing parameters effectively for an improved actuator design.

Nomenclature

A_j	=	face area vector
a	=	amplitude
b	=	plate width
C_f	=	friction coefficient
f	=	frequency
n	=	time level
p	=	pressure
r	=	jet-to-free stream ratio

¹ Research Assistant, Department of Mechanical Engineering, Gumussuyu – Istanbul / cadircis@itu.edu.tr.

² Prof. Dr., Department of Mechanical Engineering, Gumussuyu – Istanbul / guneshasa@itu.edu.tr.

³ Prof. Dr.-Ing, Institut für Aerodynamik und Gasdynamik, Pfaffenwaldring 21 / rist@iag.uni-stuttgart.de.

Re_J	= jet Reynolds number	x, X	= x -coordinate
S_a	= scaled amplitude	y, Y	= y -coordinate
S_ϕ	= source term of a scalar	Δt	= time step
St	= Strouhal number	δ	= boundary layer thickness
T	= period	δ_1	= displacement thickness
t	= time	δ_2	= momentum thickness
U_∞	= free stream velocity	δ_3	= energy thickness
u	= x -velocity of the fluid	Φ	= scalar
u_g	= velocity of the moving grid	Γ	= diffusion coefficient
v	= y -velocity of the fluid	μ	= dynamic viscosity
V	= control volume	ν	= kinematic viscosity
V_J	= jet velocity	ρ	= density
w_n	= narrow gap	τ	= shear stress
w_w	= wide gap	ω	= vorticity

I. Introduction

The active flow control devices have advantages over passive control devices since they are not fixed like passive ones and can be adapted to various flight conditions such as landing, take-off and manoeuvre¹. In the last two decades, researchers devoted their attention to the development of micro-scaled actuators that can be used to enhance the ability to control unsteady flows in and around engineering configurations such as aircrafts, nozzles, cars and marine vehicles². Various active flow control devices operating with zero-net-mass-flux system have been investigated by numerous researchers. A zero-net-mass flux actuation system that can be successfully applied to boundary layer separation at high Reynolds numbers is developed³. Additionally suction and blowing phases of a zero-net-mass flow actuator are investigated numerically to capture actuator-induced flow types⁴. A conventional vortex generator as an active zero-net-mass counterpart is demonstrated to control boundary layer separation during takeoff and landing of aircrafts⁵. A very encouraging active flow-control actuator tested in still air (e.g. wall and free jets of different orientation, vortex flow, and direct generation of vortices) is reported in detail^{6,7}.

In this study, we investigate numerically the effect of JaVA induced flows on the flat plate laminar boundary layer profiles. Previously JaVA induced flow types in still water are reported in detail^{8,9}. It is shown that JaVA has high potential for active flow control. The visualizations of JaVA-induced flows in still water and flow types with their governing parameters are reported previously, so the JaVA system used in this study originates from the previous experimental setup^{8,9}. Active flow control capability of JaVA is investigated computationally by solving time-dependent incompressible Navier-Stokes equations with appropriate boundary conditions. The boundary layer velocity profiles and other flow characteristics including the displacement thickness, the momentum thickness, the energy thickness and the friction coefficient at various operating frequencies are evaluated to demonstrate the effect of JaVA on the laminar boundary layer.

II. JaVA Model and Governing Parameters

The JaVA model is mounted in a flat plate laminar boundary layer flow as shown in Fig. 1. The JaVA is modelled as a rectangular cavity under water, and the actuator plate is placed asymmetrically with respect to the cavity opening forming a narrow (w_n) and a wide slot (w_w) between the plate and the body (see Fig. 2). The vertical motion of the actuator plate is defined by a sinusoidal velocity, thus the actuator plate moves up and down like a piston periodically with certain frequency. All of the JaVA induced flow types including periodic jets and chaotic vortices are mostly observed to emerge from the wide slot. The wide slot, the narrow slot and the actuator plate width (b) are kept constant in this study. In this study we numerically investigate the effects of the frequency on the boundary layer velocity profile keeping the amplitude of the actuator plate (a) fixed. Note that with a change in frequency, both the jet Reynolds number “ $Re_J = 2abf/\nu$ ” and the ratio of jet velocity to free stream velocity (r) changes as well. The selected frequency and the corresponding dimensionless numbers are shown in Tab. 1. Operating frequency (f) is an important parameter affecting the type of JaVA induced flows. Another important parameter affecting the flow types dramatically is the actuator plate’s mean position which denotes the location of the actuator plate with respect to JaVA cavity: it can be inside the cavity, flash-mounted with the flat plate or it can protrude over the flat plate.

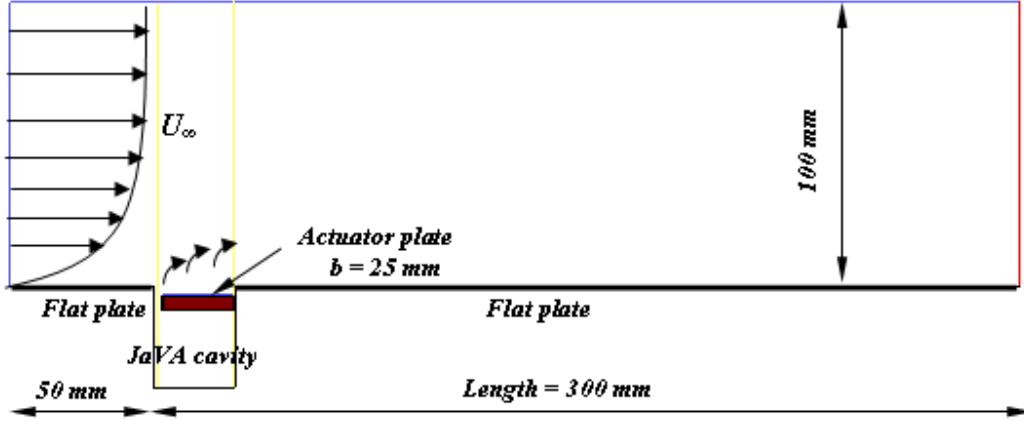


Figure 1. Schematic view of JaVA operating in a water channel

In this study the plate width is kept constant at $b = 25$ mm and the plate is inside the cavity not to disturb the free stream velocity and the JaVA induced flow-patterns. Since the plate-width is not changed, the wide gap (w_w) and the narrow gap (w_n) shown in Fig.2 have constant values 2.5 mm and 0.3 mm respectively. In this configuration, it was sufficient to reveal most of the flow features by imposing the low actuator plate frequency values between 1 and 4 Hz.

The dimensional parameters to derive non-dimensional parameters are the amplitude a [mm], the plate width b [mm] and the frequency f [Hz] of the JaVA. Thus different flow regimes can be classified in a simpler way. The scaled amplitude $S_a = 2\pi a / b$ is a dimensionless number and in this study it is kept constant, since a and b do not change. The Strouhal number of the oscillating flow is defined as $St = bf / v$ where v is the peak plate velocity of the plate ($v = 2\pi af$). With this definition, $St = b/2\pi a$ or $St = 1/S_a$. This means the Strouhal number can be substituted by scaled amplitude.

In addition to the peak plate velocity of the actuator plate, the jet velocity of the JaVA-induced flows can be defined by integrating time-averaged jet velocity over the half of the period as given in Eq. (1). One period contains blowing (ejection) and suction phases thus the integration should be over half a cycle to predict the average jet velocity of a single phase².

$$V_j = \frac{2}{T} \int_0^{T/2} v_j(t) dt = \frac{2abf}{w_w} \quad (1)$$

The jet Reynolds number (Re_j) given in Eq. (2) is derived from the volumetric flow-rate over half cycle ($T/2$) assuming that the displaced volume is equal to the product of the unit depth with the amplitude and the actuator plate width. Thus the jet Reynolds number depends on the amplitude, plate width and the frequency as

$$Re_j = \frac{V_j w_w}{\nu} = \frac{2abf}{\nu} \quad (2)$$

Another parameter necessary to interpret the effects of the JaVA-induced flow regimes in the boundary layer is the ratio of the jet-velocity to the free stream velocity. This dimensionless parameter shown in Eq. (3) is called jet-to-free stream ratio.

$$r = \frac{V_j}{U_\infty} = \frac{2abf}{w_w U_\infty} \quad (3)$$

Table 1 summarizes the dimensionless parameters based on the amplitude and frequencies. The operating conditions based on the dimensional parameters and their effects on the flow separation might be equivalent if the amplitude and the frequency are selected appropriately at constant plate width.

Table 1. The dimensionless parameters used in this study (Re_j , S_a , r).

Amplitude a [mm]	Operating frequency f [Hz]	Jet Reynolds number Re_j	Scaled amplitude S_a	Jet-to-free stream velocity r
1	1	50	0.25	0.24
	2	100	0.25	0.48
	3	150	0.25	0.72
	4	200	0.25	0.96

III. Numerical Method

A. Governing Equations

The mass and momentum conservation equations are to be solved for the investigated flow regimes. A commercial unsteady Navier-Stokes equation solver has been used to study the flows generated by JaVA in a flat plate boundary layer. Here, second order accurate finite volume schemes for pressure, and third order accurate finite volume schemes are used to discretize the governing equations. The flow is assumed to be two-dimensional to reduce the computational cost greatly. The experiments carried out in still water revealed that the two dimensional flow is justified except for the end-effects when the jet Reynolds number is high for the most JaVA-induced flow types. Thus, the continuity and momentum equations for unsteady and incompressible flow can be written as follows:

$$\frac{\partial u}{\partial x} + \frac{\partial v}{\partial y} = 0 \quad (4)$$

$$\rho \left(\frac{\partial u}{\partial t} + u \frac{\partial u}{\partial x} + v \frac{\partial u}{\partial y} \right) = -\frac{\partial p}{\partial x} + \mu \left(\frac{\partial^2 u}{\partial x^2} + \frac{\partial^2 u}{\partial y^2} \right) \quad (5)$$

$$\rho \left(\frac{\partial v}{\partial t} + u \frac{\partial v}{\partial x} + v \frac{\partial v}{\partial y} \right) = -\frac{\partial p}{\partial y} + \mu \left(\frac{\partial^2 v}{\partial x^2} + \frac{\partial^2 v}{\partial y^2} \right) \quad (6)$$

B. Computational Domain and Boundary Conditions

Based on the actuator information given before, a fine structured mesh is created reflecting all the features of JaVA acting under water. To provide an accurate solution, the grid is clustered near the actuator and in close vicinity of flat plate surface. Typical grid consists of approximately 400,000 rectangular cells and extensive grid checks have been performed. Long transients needed to be calculated before reaching steady state in the entire flow field (circa 50-120 cycles). Actuator plate motion is simulated by using a moving grid in the computational domain. As inlet boundary condition we approximate the Blasius velocity profile by 4th order polynomial given in Eq. (7). Far from the boundary layer edge we give constant free stream velocity at the upper boundary of the computational domain. In Eq. (7) δ denotes the boundary layer thickness and it is calculated using the Blasius solution. In Eq. (7) x is the distance of the wide gap from the leading edge and it is taken 1.53 m based on our experiments. In addition, in agreement with experiments, in numerical simulations we take the free stream velocity $U_\infty = 0.0838$ m/s which leads to a boundary layer thickness of $\delta = 21$ mm.

$$\frac{u}{U_\infty} = \left[2 \left(\frac{y}{\delta} \right) - 2 \left(\frac{y}{\delta} \right)^2 + \left(\frac{y}{\delta} \right)^4 \right] \quad \text{where} \quad \delta = 5 \sqrt{\frac{\nu x}{U_\infty}} \quad (7)$$

$$\frac{d}{dt} \int_V \rho \Phi dV = \frac{(\rho \Phi dV)^{n+1} - (\rho \Phi dV)^n}{\Delta t} \quad (10)$$

The volume at the $(n+1)^{\text{th}}$ time level is computed from the expression given in Eq. (11) where the first order time derivative of the control volume is computed as given in Eq. (12) to satisfy the grid conservation law. On the right hand side of Eq. (12) the sum evaluated from dot products of grid velocity by face area vector on each control volume face is equal to the volume swept out by the control volume face j over time step Δt ^{10,11}.

$$V^{n+1} = V^n + \frac{dV}{dt} \Delta t \quad (11)$$

$$\frac{dV}{dt} = \int_{\partial V} \vec{u}_g \cdot d\vec{A} = \sum_j^{n_f} \vec{u}_{g,j} \cdot \vec{A}_j \quad (12)$$

IV. Results

A. Time-Averaged and Instantaneous Flow Fields

The time-averaged velocity fields (averaged over at least 10 actuator cycles) for $f = 1, 2, 3$ and 4 Hz indicate mean velocity magnitudes in m/s. As the frequency increases, a large vortex over the plate occurs and averaged jet flow becomes more significant. As the plate is inside the cavity, the vortices emerging from wide gap continue their path in close vicinity of flat plate and have a great impact in energizing the boundary layer and delaying flow separation. This can be noticed in instantaneous vorticity fields that the vorticity is concentrated near the flat plate surface downstream of JaVA.

At high frequencies, a large vortex occurs at the top of the actuator plate. This is also observed in experiments. Instantaneous snapshots are capable to indicate how JaVA generated vortices ejected into the boundary layer. Distinct differences between ejected vortices are observable with different operating frequencies. Time-averaged flow-fields for $a = 1$ mm at various frequencies are shown in Fig. 3 and instantaneous vortex ejection and merging phenomena of the same amplitude at $f = 4$ Hz are illustrated in Fig. 4.

The velocity fields in Fig.3 are time-averaged velocity magnitudes over more than 10 cycles therefore they represent general features of the flow fields based on the operating frequency. To reveal blowing and suction phases in one period, instantaneous snapshots should be investigated closely.

In Fig. 4(a) the plate moves into the cavity to eject a jet out of the wide gap into the boundary layer ($t = 0$). As shown in Fig. 4(b) in a quarter period following the initial step ($t = T/4$) the plate continues to move further into the cavity generating two counter rotating vortices. These vortices energize the boundary layer to help delay/prevent boundary layer separation. At $t = T/2$ the plate moves upward or out of the cavity and fluid is sucked into the cavity as shown in Fig. 4(c). In Fig. 4(d) at $t = 3T/4$ suction is almost completed as one can see a big vortex forming inside the cavity which will produce new vortices for the next period. Instantaneous vorticity fields represent rotations and their directions in more detail, clockwise rotations are shown in red and counter-clockwise rotations are in deep blue. It can be clearly noticed that vortex pair moves along with jet as its strength decreases⁹.

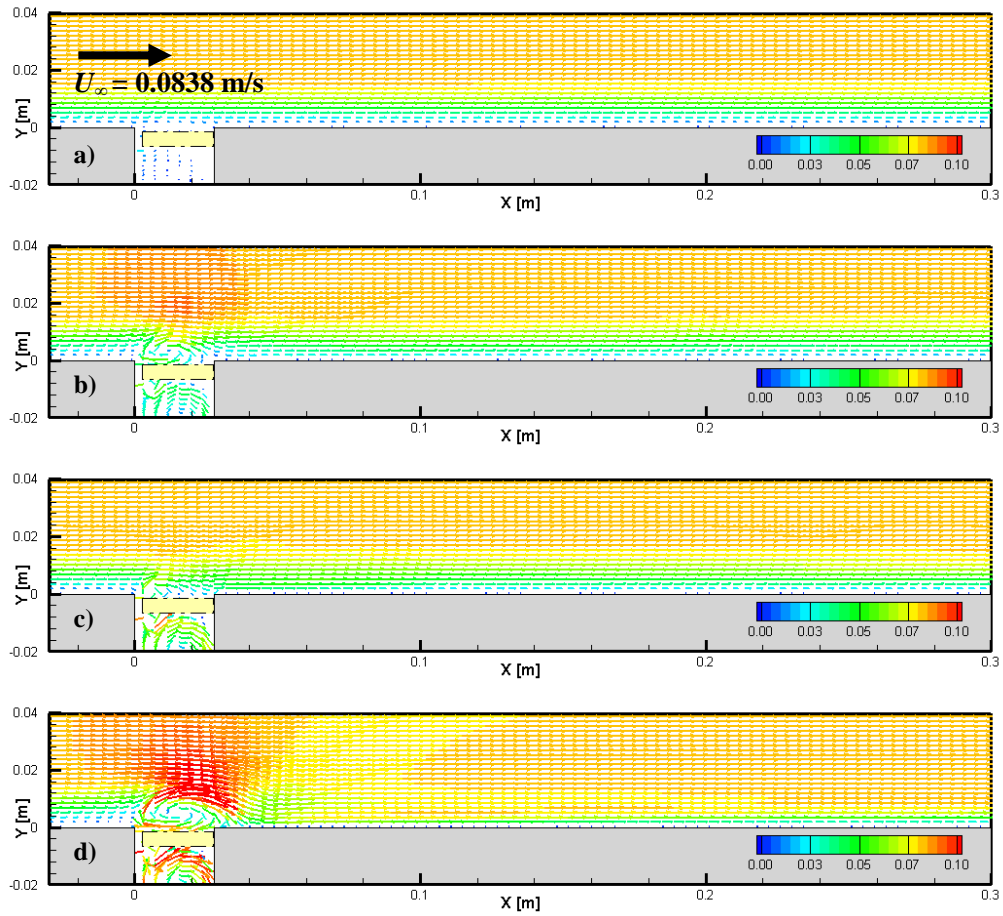


Figure 3. The time-averaged velocity fields with JaVA operating at different frequencies: JaVA parameters are $a = 1$ mm, $b = 25$ mm; a) $f = 1$ Hz, $r = 0.24$, b) $f = 2$ Hz, $r = 0.48$, c) $f = 3$ Hz, $r = 0.72$, d) $f = 4$ Hz, $r = 0.96$

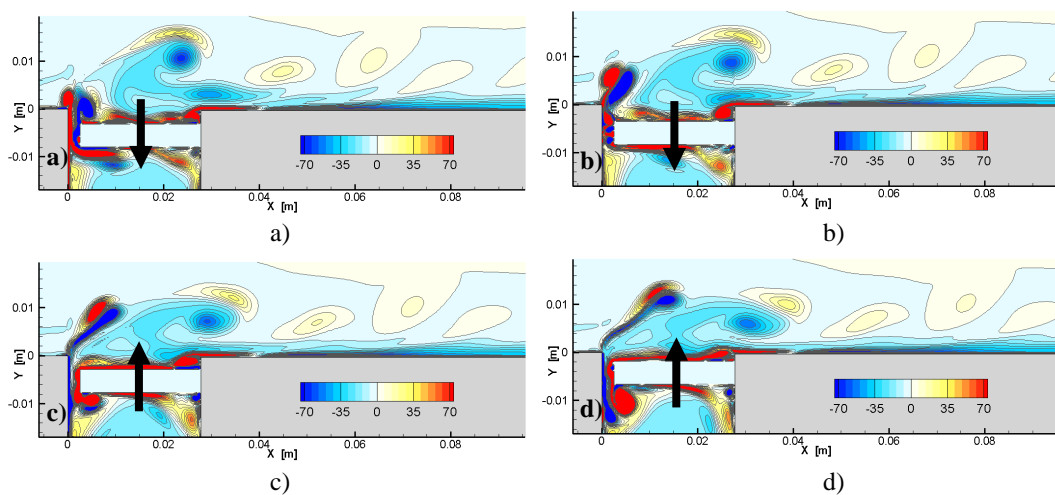


Figure 4. Instantaneous vorticity fields in one period: JaVA parameters are $a = 1$ mm, $b = 25$ mm, $f = 4$ Hz; a) $t = 0$, b) $t = T/4$, c) $t = T/2$ and d) $t = 3T/4$.

B. Time-Averaged Boundary Layer Profiles

With the increased value of frequency, the vorticity on the flat plate downstream of JaVA thickens and leads to a momentum transfer in the boundary layer. As a result, with increasing frequency, the velocity profiles are “fuller” (that is more immune to the separation) as shown at selected downstream distances in Fig. 5. Boundary layer profiles are extracted to reveal JaVA’s effects on the boundary layer at various sections in the averaged flow fields. In Fig. 5(a) averaged velocity profiles are shown in a horizontal distance of $x = 0.04$ m from the wide gap using the actuator amplitude $a = 1$ mm. Fig. 5(b), (c) and (d) indicate averaged velocity profiles in distances $x = 0.1$ m, 0.2 m and 0.3 m from the wide gap respectively. The downstream distance $x = 0.3$ m corresponds to the exit section of the computational domain with the prescribed outflow boundary condition where the boundary layer profile’s enhancement via active flow control can be observed clearly.

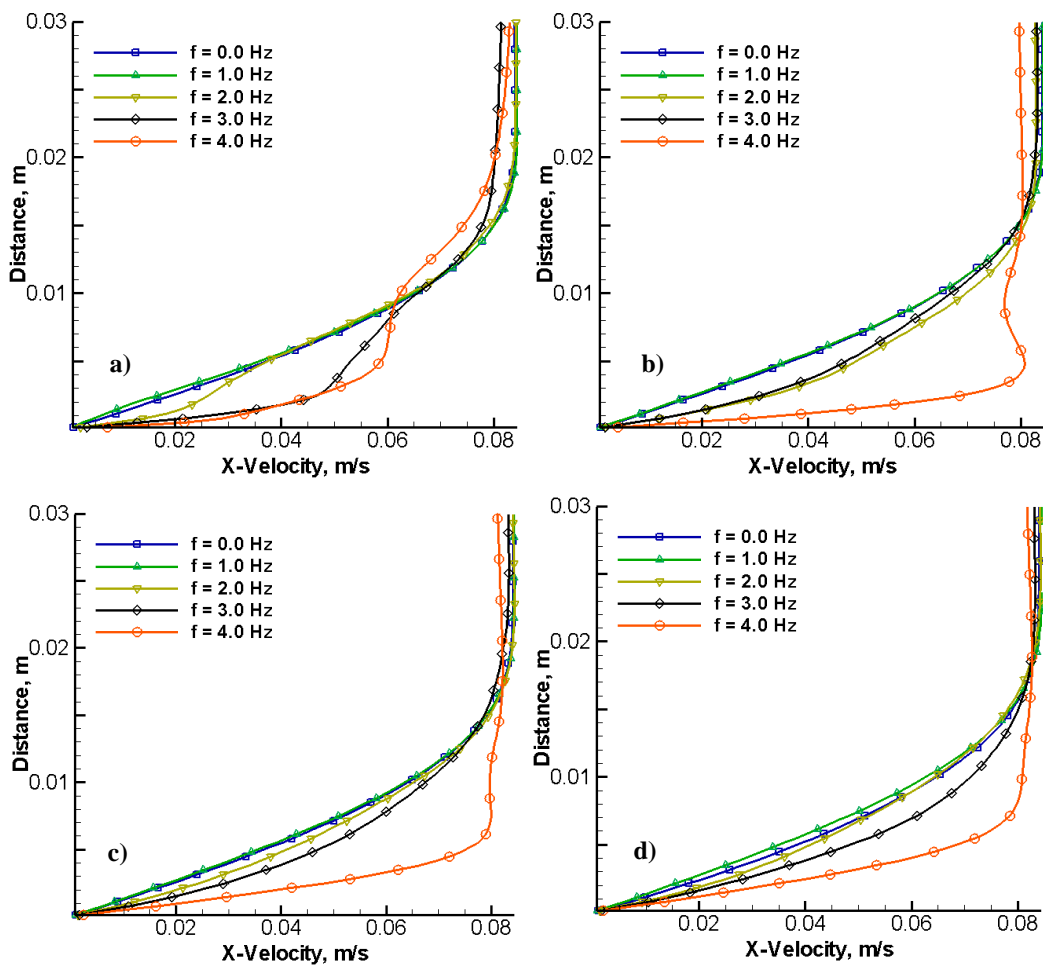


Figure 5. Time-averaged boundary layer profiles: JaVA parameters are $a = 1$ mm, $b = 25$ mm, a) $x = 0.04$ m, b) $x = 0.1$ m, c) $x = 0.2$ m and d) $x = 0.3$ m.

Fig. 5 indicates the variation of x-velocity component (downstream direction) in selected sections normal to the flat plate. It clearly shows that if actuator parameters are kept constant except for the frequency, the velocity profiles get “fuller” with increasing frequency or in other words with increasing jet-to-free stream velocity ratio. At high operating frequencies there might be local flow separation near the actuator due to low Reynolds number of the flow but this phenomenon is recovered at further sections of the flow field. The performance of JaVA in delaying flow separation highly depends on governing parameters in a way that the proper selection of the amplitude with the frequency might have different impacts on the flow.

C. Boundary Layer Characteristics

In order to reveal more information about the time-averaged boundary layer characteristics and the momentum transfer to the boundary layer, the displacement thickness, the momentum thickness, the energy thickness and the friction coefficient are calculated and their variation along the flat plate are plotted. The displacement thickness, momentum thickness, energy thickness are given as in Eqs. (13-15), respectively.

$$\delta_1 = \int_0^{\infty} \left(1 - \frac{u}{U_{\infty}}\right) dy \quad (13)$$

$$\delta_2 = \int_0^{\infty} \frac{u}{U_{\infty}} \left(1 - \frac{u}{U_{\infty}}\right) dy \quad (14)$$

$$\delta_3 = \int_0^{\infty} \frac{u}{U_{\infty}} \left[1 - \left(\frac{u}{U_{\infty}}\right)^2\right] dy \quad (15)$$

The variation of the friction coefficient can give information about the separation of the boundary layer and can be evaluated using the wall shear stress as in Eq. (16).

$$C_f = \frac{\tau_w|_{y=0}}{\rho U_{\infty}^2 / 2} \quad (16)$$

Fig. 6 shows the variation of the various boundary layer thicknesses as well as friction coefficient. As shown in Fig. 6(a) the displacement thickness decreases as the actuator frequency increases. It is also seen that the effect of JaVA is felt at far downstream of the actuator. Different from the displacement thickness, momentum and energy thicknesses increase as the operating frequency increases. In the region near JaVA the momentum and energy thicknesses at $f = 4$ Hz reach a peak point, but then the curves drop. As generally the actuator energizes more the boundary layer with increasing frequency, the momentum transfer becomes noticeable in Fig. 6(b) and (c).

With increasing actuator frequency, the friction coefficient increases as it can be seen in Fig. 6(d). Noting the fact that the customary criterion for separation point is where the shear stress (friction coefficient) becomes zero, thus the actuator is seen to delay the separation of the boundary layer. The shape factor which is the ratio of the displacement thickness to the momentum thickness supports the same finding.

V. Conclusion

A Jet and Vortex Actuator (JaVA) as an active flow control device has been investigated numerically on a flat plate boundary layer flow in a low-speed water channel. It has been shown that typical JaVA-induced flow regimes at different operating frequencies significantly energize the boundary layer thus delay boundary layer separation. The channel flow is two-dimensional, laminar and incompressible. A moving grid is required to simulate the vertical movement of actuator's plate. Instantaneous vorticity fields reveal blowing and suction phases clearly due to the motion of the actuator plate. The preliminary results show that based on the ratio of the mean jet flow to channel flow, each type of JaVA-induced jet flow produces different types of vortices in the flat plate boundary layer which considerably change the boundary layer characteristics downstream such as velocity profile, displacement thickness and friction coefficient. A general remark on JaVA's performance at different operating conditions is that highest frequency enhances the boundary layer mostly. This numerical study reveals that JaVA has a high potential to modify the boundary layer profiles in a way that the flow separation can be delayed or prevented for long downstream distances. A desired outcome of the interaction of the JaVA induced vortices with the boundary layer flow depends on many geometric and operating conditions (JaVA and free stream velocity) which must be appropriately chosen.

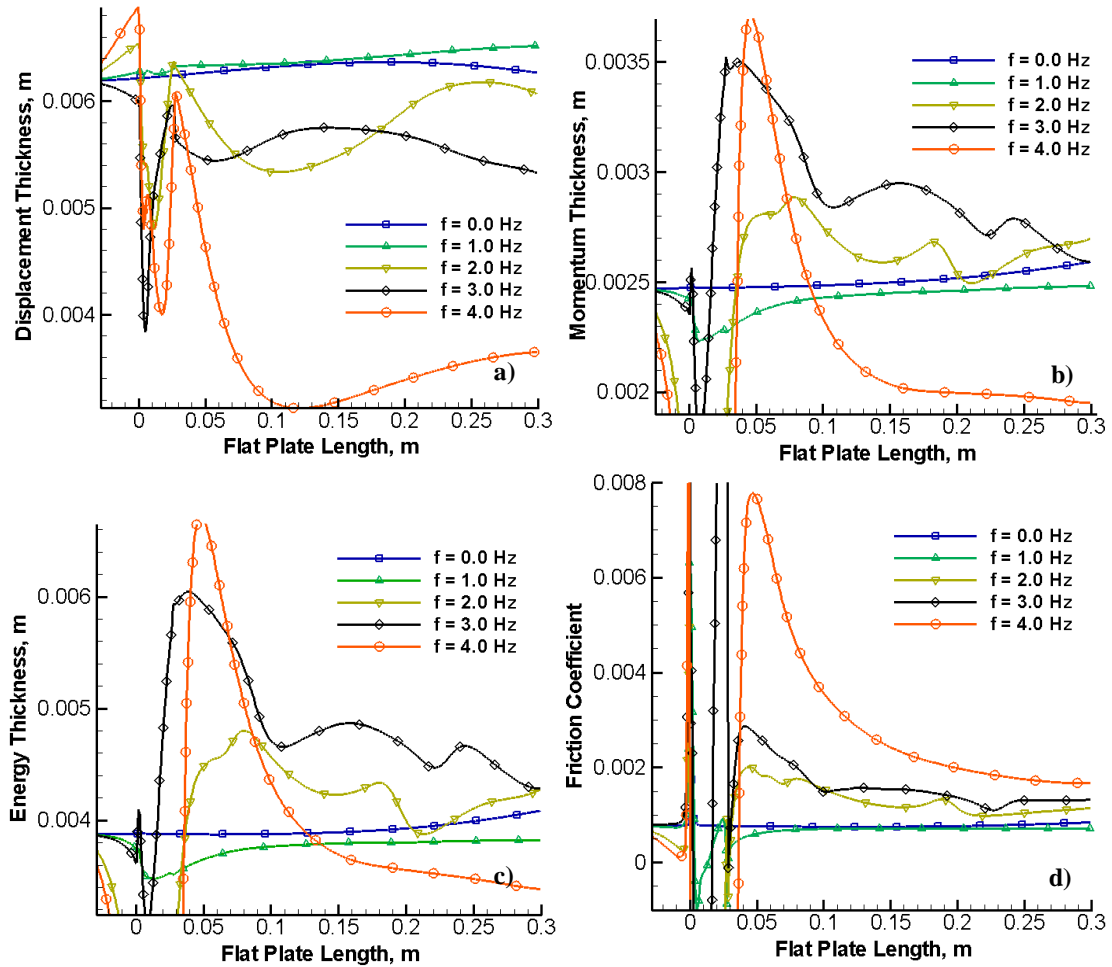


Figure 6. Variation of boundary layer characteristics: a) δ_1 , b) δ_2 , c) δ_3 and d) C_f .

Acknowledgments

We gratefully acknowledge the financial support of Scientific and Technical Research Council of Turkey (TÜBİTAK) and International Bureau of the Federal Ministry of Education and Research (BMBF), Germany through the project “Development and Testing of a Jet and Vortex Actuator (JaVA) for Active Flow Control”, Nr. 107M644 and TUR 07/006, respectively.

References

- ¹Gad-el-Hak, M., *Flow Control- Passive, Active and Reactive Flow Management*, Cambridge University Press, 2006.
- ²Joslin, R. D., Lachowicz, J. T., and Yao C., “DNS of Flow Induced by a Multi-Flow Actuator,” *Proceedings of ASME Fluids Engineering Division Summer Meeting, FEDSM’98*, ASME, Washington, DC, 1998.
- ³Seifert, A., and Pack, L., “Oscillatory Control of Separation at High Reynolds Numbers,” *36th Aerospace Sciences Meeting and Exhibit*, AIAA 98-0214, Reno, Nevada, 1998.
- ⁴Kral, L. D., Donovan, J. F., Cain, A. B., and Cary, A. W., “Numerical Simulation of Synthetic Jet Actuators,” *28th AIAA Fluid Dynamics Conference*, AIAA 97-1824, Snowmass Village, Colorado, 1997.
- ⁵Johnston, J. P., and Nishi, M., “Vortex Generator Jets-A Means for Separation Control,” *AIAA Journal*, Vol. 28, No. 6, 1990, pp. 989-994.
- ⁶Lachowicz, J. T., Yao C., and Wlezien, R. W., “Physical Analysis and Scaling of a Jet and Vortex Actuator,” *Proceedings of the 3rd ASME/JSME Joint Fluids Engineering Conference, FEDSM’99-6921*, ASME, San Francisco, California, 1999.

⁷Lachowicz, J. T., Yao, C., and Wlezien, R. W., "Flow Field Characterization of a Jet and Vortex Actuator," *Experiments in Fluids*, Vol. 27, 1999, pp. 12-20.

⁸Gunes, H., Cadirci, S., Baldani, F., Peters, B., and Rist, U., "Temporal Analysis of Jet and Vortex Actuator (JaVA)-induced Flows," *International Conference on Jets, Wakes and Separated Flows*, ICJWSF, Berlin, Germany, 2008.

⁹Gunes, H., Cadirci, S., and Rist, U., "Experimental Investigation of Jet and Vortex Actuator Using Particle Image Velocimetry," *ASME International Mechanical Engineering Congress & Exposition*, ASME-IMECE2009-11451, Orlando, Florida, 2009.

¹⁰Rashad, M. A., "CFD Simulation of Jet and Vortex Actuators (JaVA) with and without Cross Boundary Layer," Ph.D. Dissertation, IAG-Universität Stuttgart, 2010.

¹¹Fluent Inc.: FLUENT 6.3 User's Guide. Documentation, 2008.